Reference 51

Experimental characterization of the reflectance of 60° waveguide bends in photonic crystal waveguides

M. H. Shih,[a] Woo Jun Kim, Wan Kuang, J. R. Cao, Sang-Jun Choi, John D. O'Brien, and P. Daniel Dapkus
Department of Electrical Engineering-Electrophysics, University of Southern California, Powell Hall of Engineering, 3737 Watt Way, Los Angeles, California 90089-0271

(Received 17 January 2005; accepted 16 March 2005; published online 3 May 2005)

Photonic crystal waveguides with two 60° bends were fabricated in an InGaAsP/InP suspended membrane geometry. The transmission spectrum was measured and the reflectance of the 60° bend was evaluated from Fabry–Perot oscillations using Fourier analysis. It is shown that the reflectance agrees well with the results of a finite element method simulation.
 [DOI: 10.1063/1.1923169]

Planar photonic crystal waveguide (PCWG) technology has the potential to be a fundamental building block for future optical integrated circuits. Some of this potential arises from the ability to form small turning radius waveguide bends and wide angle *Y* branches[1–4] leading to the possibility of dense device integration. There have been many experimental demonstrations of two-dimensional (2D) PCWGs and, recently, low loss PCWGs have been reported.[5–7] There have also been a few demonstrations published to date of PCWG bends.[1,3] However, ultralow loss junctions have only recently been reported.[8] In this letter, we report on a technique to determine the reflection at photonic crystal junctions and demonstrate high transmittance of a single-defect line doubly bent waveguide structure formed in a suspended two-dimensional photonic crystal membrane.

The doubly bent waveguides were fabricated in an InP/InGaAsP membrane. The waveguides were formed by a single-line defect in a 2D triangular lattice photonic crystal. The InGaAsP membrane in the finished devices was 240 nm thick. A range of path lengths between the waveguide bends, L_{Bend}, was fabricated as shown in Fig. 1. Open areas were defined outside of the PCWG cladding in these devices in order to facilitate the formation of suspended membranes. L_{Bend} was along the Γ-K direction and its value varied between 21.42 μm (50 periods), 31.92 μm (75 periods), and 42.42 μm (100 periods) for this work. The details of fabrication process have been discussed in our previous work.[9] The devices reported here have a lattice constant, a, of 420 nm and hole radius to lattice constant ratio, r/a, around 0.3. The waveguides had ten periods of photonic crystal cladding on each side of waveguide core.

Since the reflectance of the bend is not zero within the measured wavelength region, we expect that the optical intensity transmitted through the waveguides will exhibit Fabry–Perot oscillations as a function of the frequency with a period that depends inversely on the length of the sections between the waveguide bends. By looking for oscillations in the transmitted intensity with the expected period, we can extract information about the properties of the waveguide bends.

A 2D finite element method[10] was used to calculate the transmission of the straight waveguide and a waveguide with a single bend for the r/a value, 0.3. Figure 2(a) shows the simulated transmission, where the gray-dashed line is the transmission spectrum of the straight waveguide, and the black-solid line is the transmission spectrum of the bent waveguide. This model is a 2D calculation using an effective index for the waveguide mode. Selected points on these curves were checked with a three-dimensional simulation, however. An external source was used in the finite element calculation, and the reduction of the theoretical transmission at longer wavelengths in this figure is due to the decreasing coupling efficiency between the source and the waveguide near the waveguide band edge.

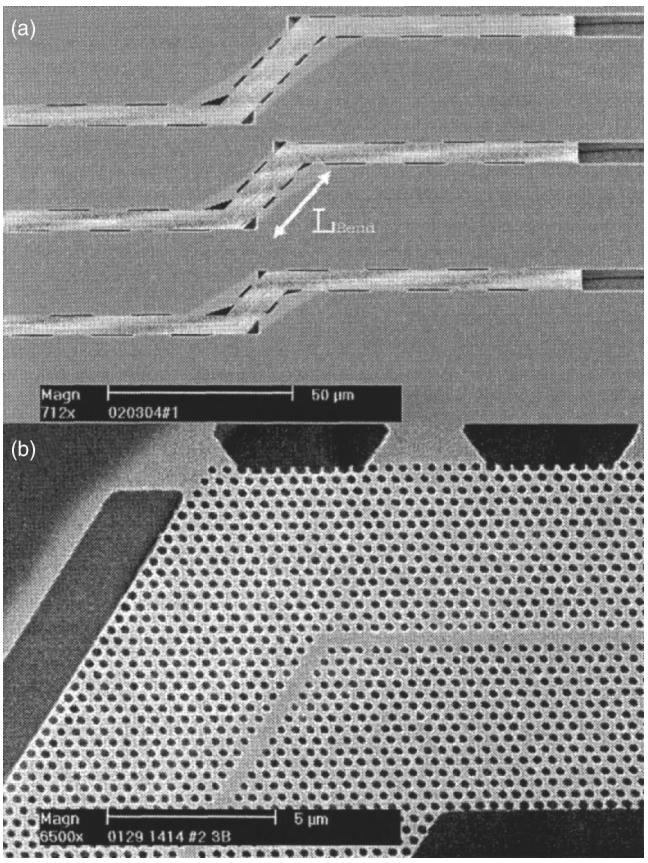

FIG. 1. (a) Scanning electron micrograph showing parts of three doubly bent PCWGs with the different waveguide lengths between the bends. (b) A magnified view of a 60° waveguide bend.

[a]Electronic mail: minhsius@usc.edu

Report Documentation Page

Form Approved
OMB No. 0704-0188

1. REPORT DATE	2. REPORT TYPE	3. DATES COVERED
01 JUN 2005	**N/A**	**-**

4. TITLE AND SUBTITLE	5a. CONTRACT NUMBER
Experimental characterization of the reflectance of 60° waveguide bends in photonic crystal waveguides	5b. GRANT NUMBER
	5c. PROGRAM ELEMENT NUMBER
6. AUTHOR(S)	5d. PROJECT NUMBER
	5e. TASK NUMBER
	5f. WORK UNIT NUMBER
7. PERFORMING ORGANIZATION NAME(S) AND ADDRESS(ES) **Department of Electrical Engineering-Electrophysics, University of Southern California, Powell Hall of Engineering, 3737 Watt Way, Los Angeles, California 90089-0271**	8. PERFORMING ORGANIZATION REPORT NUMBER
9. SPONSORING/MONITORING AGENCY NAME(S) AND ADDRESS(ES)	10. SPONSOR/MONITOR'S ACRONYM(S)
	11. SPONSOR/MONITOR'S REPORT NUMBER(S)

12. DISTRIBUTION/AVAILABILITY STATEMENT
Approved for public release, distribution unlimited

13. SUPPLEMENTARY NOTES
See also ADM001923.

14. ABSTRACT

15. SUBJECT TERMS

16. SECURITY CLASSIFICATION OF:			17. LIMITATION OF ABSTRACT	18. NUMBER OF PAGES	19a. NAME OF RESPONSIBLE PERSON
a. REPORT	b. ABSTRACT	c. THIS PAGE			
unclassified	**unclassified**	**unclassified**	**UU**	**3**	

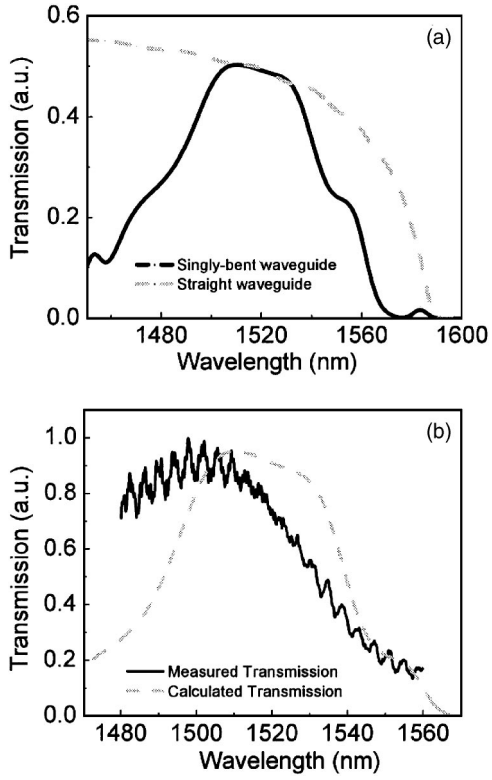

FIG. 2. (a) The calculated transmission spectra of a single-line defect PCWG (dashed lines) and a single-bent PCWG (solid line). (b) The comparison of the measured spectrum (black line) and simulated spectrum (gray line) of the doubly bent waveguides.

The experimental transmission spectra were measured using a tunable laser. The objective lens used to launch the signal into the waveguides had a numerical aperture of 0.55. A spatial filter was used at the output to exclude light that did not pass through the PCWG. The output intensity was collected by a cooled InGaAs detector. The comparison of the measured and simulated spectra for the doubly bent waveguide is shown in the Fig. 2(b). The gray line is the simulated transmission spectrum of the doubly bent structure with an r/a value of 0.30 and the black line is the measured transmission of the doubly bent structure with an r/a value that is slightly larger than 0.30. The measured data exhibits good agreement with the theory.

We observed oscillations in the transmitted intensity spectra of these waveguides that have a period that varies inversely with the length of the waveguide section between the bends, as expected. Figures 3(a) and 3(b) are the two measured spectra from two of the doubly bent photonic crystal waveguides with bending section lengths of 42.42 μm and 21.21 μm. By filtering out the high-frequency contributions, which are due to longer sections of these bent waveguide structures and the oscillation of the tunable laser, we can pick up the peak-to-valley ratio, K, of the oscillations due to the resonance formed between the waveguide bends. Figure 3(c) shows one of measured spectra at this stage. The reflectance, R, of the photonic crystal bend was extracted using the following formula[11]

$$R = \left(\frac{\sqrt{K}-1}{\sqrt{K}+1}\right) 10^{(\alpha_{\mathrm{dB}} L_{\mathrm{Bend}}/10)}, \tag{1}$$

where α_{dB} is the propagation loss of the waveguide. Figure 3(d) shows the reflectance R of the 60° bend extracted from

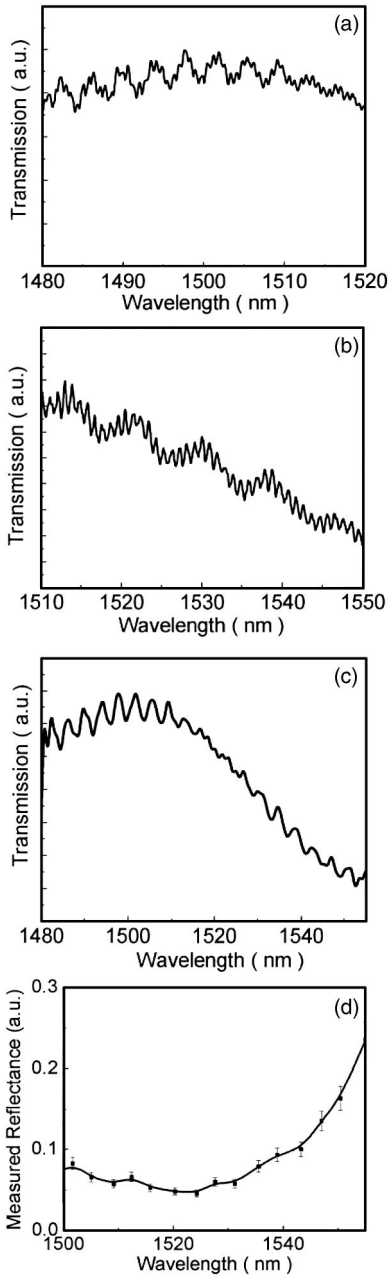

FIG. 3. The measured transmission spectrum of the doubly bent waveguide with bending section length of (a) 42.42 μm and (b) 21.21 μm. (c) The transmission spectrum of (a) after numerically filtering the oscillations due to reflection of facets and the tunable laser. (d) The reflectance of the 60° photonic crystal bend extracted from the transmission spectrum in (c).

the data in Fig. 3(c). Since the bending section lengths L_{Bend} are small, we expect the reflectance R to be nearly insensitive to the propagation loss α_{dB} of the waveguides. The error bars in Fig. 3(d) represent the variation of the reflectance R due to the range of propagation loss α_{dB} values, from 2 to 20 dB/mm. A wavelength region of low reflectance is observed around the wavelength 1520 nm. This is also obvious from the small amplitude oscillations in Fig. 3(c). The measured and simulated reflectances are compared in Fig. 4. Figure 4(a) shows the measured reflectance of the 60° bend as a function of wavelength. The three lines are for r/a values of 0.305 (star points), 0.31 (triangular points), and 0.32 (square points), respectively, and Fig. 4(b) shows the simulated reflectance of the 60° photonic crystal bend. This curve is calculated from the model transmission spectrum

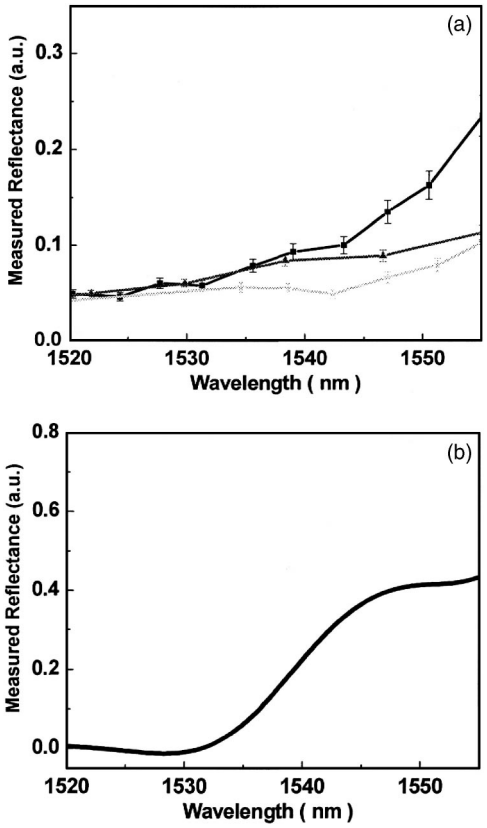

FIG. 4. (a) The reflectances calculated from the measured spectra with different r/a values, 0.305(star-point line), 0.31(triangular-point-line), and 0.32(square-point line). The error bars represent the range of the reflectance extracted due to the range of propagation loss values from 2 dB/mm to 20 dB/mm. (b) The simulated reflectance spectrum extracted from the transmission spectrum in Fig. 2(a).

shown in Fig. 2(a). In Fig. 4(a), the measured reflectance increases as the guided wavelength increases, and as the r/a values increases. This trend is predicted by the theoretical model. The lowest measured reflectance value of 5% over the wavelength region from 1520 nm to 1535 nm implies that the transmission of the photonic crystal 60° bend is about 95%. Since the long-wavelength region is close to the band edge of the guided band of the doubly bent PCWG, the transmitted power is small because of the large impedance mismatch between the input beam and guided wave. It is therefore not reliable to extract reflectance information in this low intensity region. The region of comparison in Figs. 4(a) and 4(b) is then the shorter-wavelength region between 1520 nm and 1545 nm. The smallest measured reflectance is slightly larger than that predicted by our model, and we attribute this difference to fabrication imperfections in our measured waveguides.

In summary, we have observed 95% transmittance through the doubly bent single-line defect photonic crystal suspended membrane waveguides over a bandwidth of 15 nm. The reflectance of the 60° bend were extracted both from measured and simulated spectra. We obtained good agreement between the measured spectra and the finite element method numerical model.

This study is based on research supported by the Defense Advanced Research Projects Agency (DARPA) under Contract No. F49620-02-1-0403 and by the National Science Foundation under Grant No. ECS-0094020. Computation for the work described in this letter was supported, in part, by the University of Southern California Center for High Performance Computing and Communications.

[1] E. Chow, S. Y. Lin, J. R. Wendt, S. G. Johnson, and J. D. Joannopoulos, Opt. Lett. **26**, 286 (2001).
[2] Y. Sugimoto, N. Ikeda, N. Carlsson, K. Asakawa, N. Kawai, and K. Inoue, J. Appl. Phys. **91**, 3477 (2002).
[3] A. Talneau, L. L. Gouezigou, N. Bouadma, M. Kafesaki, C. M. Soukoulis, and M. Agio, Appl. Phys. Lett. **80**, 547 (2002).
[4] A. Sharkway, D. Pustai, S. Shi, and D. W. Prather, Opt. Lett. **28**, 1197 (2003).
[5] S. J. McNab, N. Moll, and Y. A. Vlasov, Opt. Express **11**, 2927 (2004).
[6] Y. Sugimoto, Y. Tanaka, N. Ikeda, H. Nakamura, K. Asakawa, and K. Inoue, Opt. Express **12**, 1090 (2004).
[7] M. Notomi, A. Shinya, S. Mitsugi, E. Kuramochi, and H.-Y. Ryu, Opt. Express **12**, 1551 (2004).
[8] L. H. Frandsen, P. I. Borel, Y. X. Zhuang, A. Harpoth, M. Thorhauge, M. Kristensen, W. Bogaerts, P. Dumon, R. Baets, V. Wiaux, J. Wouters, and S. Beckx, Opt. Lett. **29**, 1623 (2004).
[9] M. H. Shih, W. J. Kim, W. Kuang, J. R. Cao, H. Yukawa, S. J. Choi, J. D. O'Brien, and P. D. Dapkus, Appl. Phys. Lett. **84**, 460 (2004).
[10] W. J. Kim and J. D. O'Brien, J. Opt. Soc. Am. B **21**, 289 (2004).
[11] J. Zimmermann, M. Kamp, R. Schwertberger, A. Forchel, and R. Marz, IEEE Electron. Lett. **38**, 178 (2002).